ISSN 2176-5480

22nd International Congress of Mechanical Engineering (COBEM 2013)
November 3-7, 2013, Ribeirão Preto, SP, Brazil

EXPERIMENTAL INVESTIGATION OF TURBULENT JET FLOW FROM A CHEVRON NOZZLE

Lígia Venancio Froening
Cesar Jose Deschamps
Juan Pablo de Lima Costa Salazar
Universidade Federal de Santa Catarina, Florianópolis –SC, Brasil.
ligia@polo.ufsc.br
deschamps@polo.ufsc.br
juan.salazar@ufsc.br

Carlos Roberto Ilário da Silva
EMBRAER S.A., São José dos Campos –SP, Brasil
carlos.ilario@embraer.com.br

Abstract. *This paper presents hot-wire measurements of the flow field of a subsonic jet exiting from a chevron nozzle at different Mach numbers. The potential core length, spreading rate, as well as axial and radial turbulence profiles are compared to those from a baseline case of a circular nozzle without chevrons. Modifications to jet velocity profiles produced by chevron nozzles are known to shift the noise spectrum to higher frequencies, thereby reducing noise levels for distant observers. In this context, the turbulent flow is explored in an attempt to uncover underlying jet noise reduction mechanisms generated by chevron nozzles.*

Keywords: *Jet flow, chevron nozzle, turbulence, aeroacoustics.*

1. INTRODUCTION

The aviation industry has always faced challenges because of its fast growth. More recently, urban areas have begun to encroach on areas originally reserved to airports and, as a consequence, aircraft-generated noise has become a significant problem. The technological advances arising from massive investments in research yielded noise reduction higher than 30dB (Silva, 2011). The high velocity jet from the engines is one of the dominant noise generating mechanisms, especially at landing and take-off. Hence, much effort has been focused on finding solutions to the jet noise problem. Chevron nozzles are passive noise devices that have proven to be a viable option when taking into account the trade-off between noise reduction and loss of thrust.

Jet flow has been experimentally investigated via hot wire anemometry (HWA) and particle image velocimetry (PIV). HWA can provide single-point measurements at high acquisition rate, enabling spectral analysis of the turbulent flow. On the other hand, PIV is capable of measuring the unsteady flow field in sequential frames. However, the highest frequency is limited to approximately 25 kHz (Wernet, 2007).

Recently, Morris and Zaman (2010) have adopted one and two-dimensional HWA probes to obtain statistical properties of jets, mainly those related to acoustic noise, such as axial and radial velocity components, turbulence intensity, second and fourth order cross correlations, length scales and power spectral density. They observed that the characteristics of the statistical properties are very similar in the regions of highest turbulent velocity fluctuations. This provides some basis for similarity assumptions adopted by statistical models to estimate noise sources. Morris and Zamma (2010) also found a significant variation of length scales with Strouhal number and recommended to take this variation into account in prediction model so as to capture the physics of noise generation.

The effects of chevron nozzles on the acoustic field have been widely studied. Bridges and Brown (2004) analyzed the influence of chevron nozzle geometric parameters on the flow and acoustic fields. They showed that chevron nozzles give rise to axial vorticity, increasing the mixing layer growth rate into the potential core. In the case of closely spaced chevrons, Bridges and Brown (2004) observed that vortices have a trend to destroy the others and that this process reduces radial transport. Chevrons were not seen to reduce overall acoustic noise level, but to shift noise from lower to higher frequencies in the spectrum. Chevron penetration was identified as the most relevant parameter, allowing a reduction of 3-5 dB at low frequencies for certain positions of the observer.

Callender *et al*. (2010) performed PIV measurements of jets originated by four different nozzles and confirmed that chevron penetration affects the mixing intensity, which is related to the sound generation mechanism. Larger penetration produces greater reductions of noise at low frequencies but also increases it at high frequency. The authors concluded that there are two fundamental physical mechanisms induced by chevrons nozzles. The first is the enhanced mixing that increases the decay rate of the potential core, reducing jet noise near the range of the frequency peak. The second mechanism is the increase of turbulence in the shear layer that generates high frequency noise.

Engel (2012) carried Reynolds Averaged Naviers-Stokes (RANS) simulations of jet flow for three nozzle geometries used by Bridges and Brown (2004). Predictions of the acoustic field was also obtained by using the

ISSN 2176-5480

commercial software CAA++ together with the waveprop1 feature, from Metacomp Tech. Good agreement was found between predictions and experimental data for the flow field. However, differences of up to 20dB were verified in the results for sound pressure levels (SPL). This shortcoming of the model was attributed to its failure to properly reconstruct the random turbulence field from the result of the mean flow field.

The present work is part of a research project devised to study jet noise. This paper reports HWA measurements acquired in an experimental setup developed to investigate turbulence mechanisms behind the acoustic modifications introduced by chevrons. Additionally, the work has also the objective of providing data to support the validation of new predictions models. Velocity profiles were measured at different locations so as to identify differences in the velocity and turbulence fields brought about by a chevron nozzle (SMC006) in relation to a baseline nozzle (SMC000) without chevron. The Mach and Reynolds numbers of such tests are 0.13 and 35 000, respectively.

2. EXPERIMENTAL SETUP AND PROCEDURE

2.1 Experimental setup

A small jet rig, for academic purpose, was projected and built using the Small Hot Jet Acoustic Rig (SHJAR) described by Bridges and Brown (2005) as the main reference. The design of the test rig fulfills the following requirements:

i) study of single and unheated jets;
ii) use of available infrastructure;
iii) investigation of the flow field.

The air supply system is composed of two compressors with 566 l/min and 1640 l/min of capacity and 8 bar of pressure, an air dehumidifier and three 500 l storage tanks. The rig is equipped with valves for flow rate control, pressure and temperature transducers, a turbine flow meter, together with equipment to characterize the jet flow itself (Figure 1).

Figure 1 – Schematic of jet rig apparatus (1. Filter; 2. Pressure valve; 3. Precision flow control valve; 4. Flow meter; 5. Flow Straightener, Pressure and temperature probe).

ISSN 2176-5480

Air flows through a pipe with diameter of 19.05 mm from the storage tanks up to the flow meter. After this position, the pipe diameter is enlarged twice, firstly to a 38.31 mm and then to 88,90 mm. A flow straightener is then used at this low speed condition and temperature and pressure are measured. Before reaching the nozzle, the pipe is again contracted to a 38.31 mm diameter.

The selected nozzles, as mentioned above, were SMC000 and SMC006 (Figure 2). Since penetration was shown to be the most important parameter, the SMC006 nozzle was selected between 10 other chevron nozzles studied by Bridges and Brown (2004). The SMC000 is considered the baseline nozzle and has the same geometry as the others, albeit without chevrons. The main characteristics of SMC006 are:

i) number of chevrons: 6;
ii) chevron length: 5.65 mm;
iii) angle (given by angle to jet centerline): 18.2º;
iv) penetration (difference in radius from tip to base of the chevron): 0.881 mm.

Figure 2 - SMC000 and SMC006 nozzles.

The hot wire anemometry system, from Dantec Dynamics, has two CTA (constant temperature anemometer) modules, model 90C10, for velocity measurement, one CCA (constant current anemometer) module, model 90C20, for temperature measurement and a velocity calibration unit, model 90H10. All modules are controlled by a central unit (StreamLine 90N10). The measurements were carried out using the miniature wire-probe type 55P11.

2.2 Experimental procedure

An automatic 3-axis traverse was used to move the probe to the measurement positions inside the jet. The probe was aligned with the jet axis by using a laser beam and mirror. A special stem was designed to exactly match the Dantec Dynamics original probe support so it could be attached to a micrometer table, as shown in Figure 3.

Preliminary measurements were made over planes at several downstream positions of the nozzle exit. A Gaussian surface (Figure 4) was fitted to measurements on each plane. This procedure gave an estimate of the location of the jet centerline and guided positioning of the traverse for subsequent measurement campaigns.

Figure 3 - Detailed image showing the probe support.

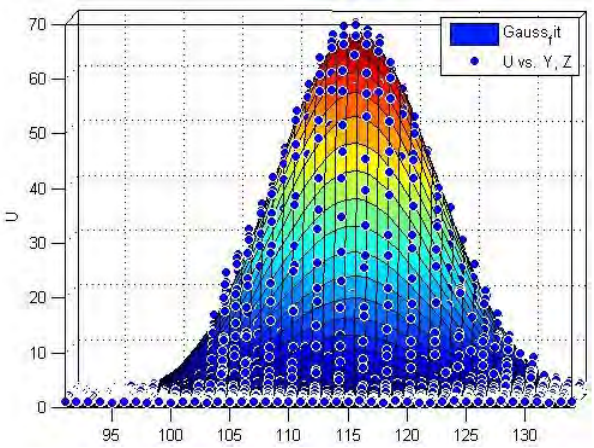

Figure 4 – Gaussian fit of velocity profile

The jet exit velocity was controlled by two valves: i) a pressure-regulating valve to keep the flow rate constant; ii) a needle valve for fine adjustments. Signals from the thermocouples, pressure transducer and flow meter were acquired by a National Instruments system and monitored via a acquisition code developed with Labview. The National

ISSN 2176-5480

Instruments system is composed by an A/D border model PCI-6071E, an I/O connector block model SCB-100 and a low-noise chassis SCXI-1000 that holds up two modules, the SCXI-1302 and SCXI- 1303. The acquisition system was also used to monitor flow stability and fluid properties. Measurements were recorded only after steady state flow condition was reached.

The jet exit velocity (U_j) was calculated by averaging the velocity measurements made along vertical and horizontal lines through the jet center at approximately 3 mm downstream of the nozzle tip. Table 1 shows relevant parameters for each experiment. Free jets will asymptotically tend to a self-similar profile that results in analytical solutions to the flow governing equations. Therefore, the initial experiment (A) served the purpose of establishing a baseline case as well as verifying agreement with the large body of jet results published in the literature, thereby validating the rig and measurement procedures. In the second experiment (B), modifications to the flow generated by the chevron nozzle were investigated.

Table 1 – Measurement runs

	Units	**Exp. A**	**Exp. B**
Nozzle type	-	SMC 000	SMC 006
Nozzle Diameter	[mm]	12.5	11.83
Exit Velocity	[m/s]	43.27	45.37
Standard Deviation	[m/s]	1.071	0.551
Volumetric Flux	[m^3/s]	0.00531	0.00499
Momentum Flux	[m^4/s]	0.2298	0.2262
Jet Reynolds Number	-	35 300	35 100
Mach Number	-	0.13	0.13

3. RESULTS

3.1 Classical Jet Analysis

The radial velocity profile from the SMC000 nozzle at several downstream positions is shown in Figure 5. At the nozzle exit, the velocity profile is approximately a top-hat, with a well-defined exit velocity (U_j). As the jet evolves downstream from nozzle, it spreads and the centerline velocity decays.

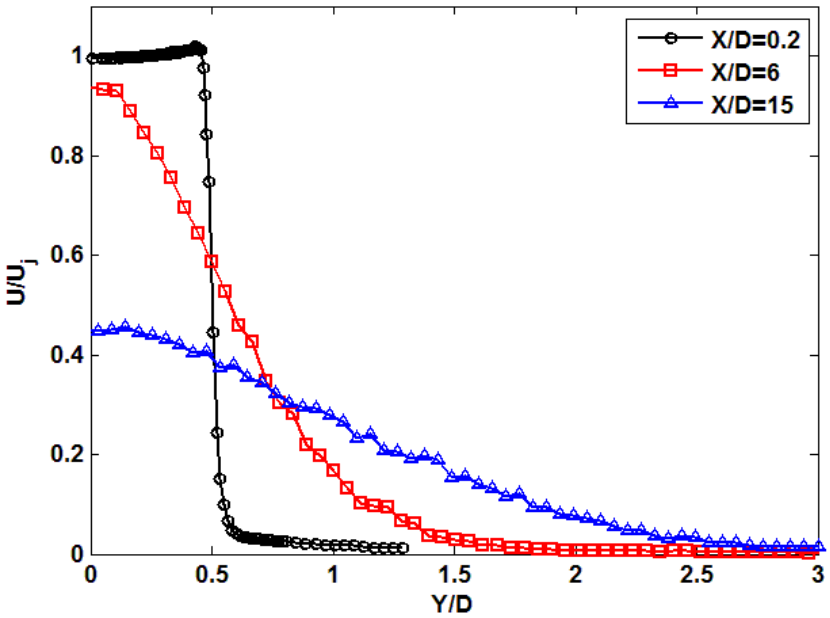

Figure 5 – Radial Velocity Profile

ISSN 2176-5480

The potential core is a region of the jet that extends up to 4.5 *D* in the downstream direction where the velocity remains the same as the exit velocity. A shear layer evolves around the potential core, generating large radial velocity gradients and turbulence intensity. This extension along with a transition region is commonly referred as development region. In the development region, the jet accommodates the initial conditions particular to each case, after which the radial profile, reaches the so-called self-preserving state (or similarity region). George (1989) defines the similarity as the region where the profiles of velocity or any other quantity can be brought into congruence by simply scaling it using a factor dependent on only one of the variables. As a consequence, the governing equations become independent of that variable and for a symmetric jet, this means a reduction into ordinary differential equations, allowing analytical solutions. However, at real conditions, the jet only tends asymptotically to this state and, as discussed by George (1989), it may not be completely independent of initial conditions. Pope (2000), analyzing data from Wygnanski and Fielder (1969) data, considered this self-preserving state to happen at distances up to 30 *D*. The mean axial velocity plot for six different positions obtained in experiment A can be seen in Figure 6. These results agree with the reference value of 30 *D* for the development length.

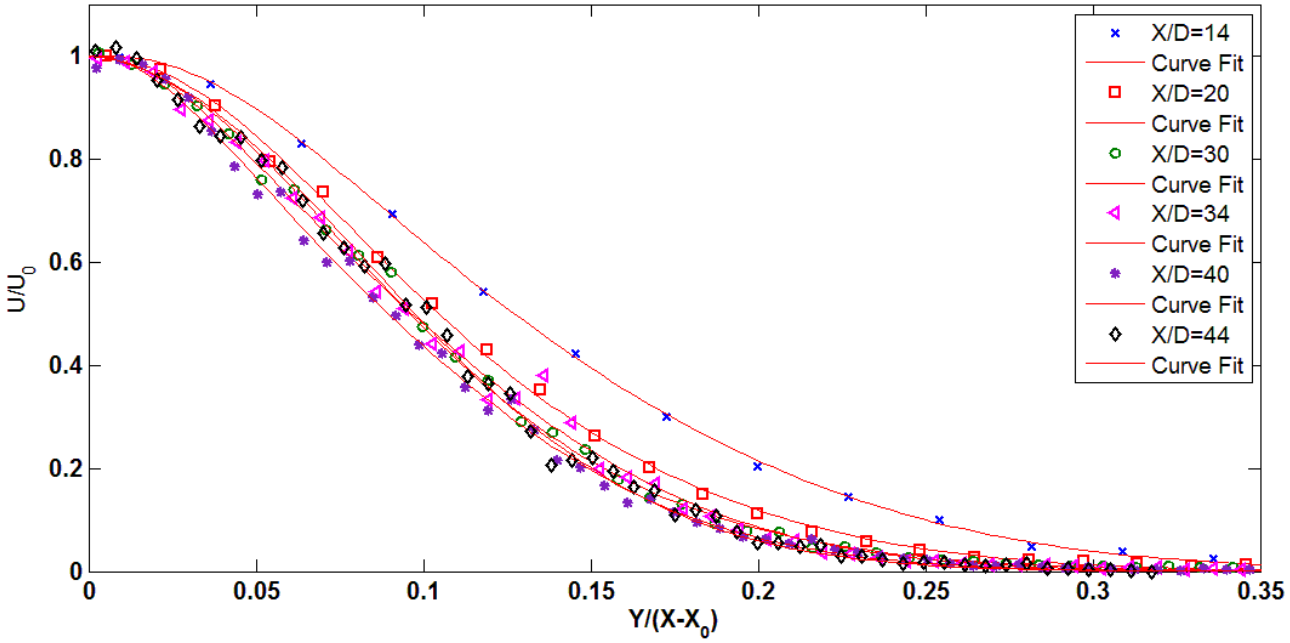

Figure 6 – Normalized Radial Profile of Mean Axial Velocity in a Round Jet (Baseline Nozzle)

The centerline velocity U_0 used to scale the coordinate axis is defined by (Eq. 3):

$$U_0(x) = \langle U(x,0,0) \rangle \tag{3}$$

and was calculated from the Gaussian fit of the velocity profile obtained at each measurement plane. The variable $\eta = y/(x-x_0)$, used as the abscissa, is a function of the downstream position (x). The virtual origin x_0 is defined in the following paragraphs.

When the flow reaches a self-similar state, it becomes almost independent of its initial conditions. Thus, one expects parameters like the spreading rate and the decay rate to be the same in all jets. The decay rate can be analyzed with the aid of Eq. 4,

$$\frac{U_j}{U_0} = \frac{1}{B_u}\left[\frac{x}{D} - \frac{x_0}{D}\right] \tag{4}$$

Figure 7 – Centerline Velocity Variation with Distance from JetFigure 7 shows a plot of U_j/U_0. The virtual origin is given by the value where the projection of the curve fit, intercepts the x-axis, *D* is the exit nozzle diameter, and the decay constant B_u is the inverse of the slope of the same curve.

ISSN 2176-5480

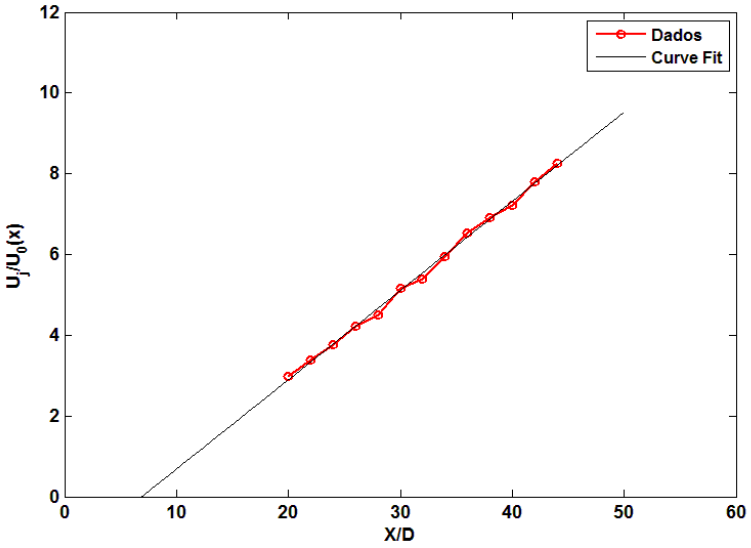

Figure 7 – Centerline Velocity Variation with Distance from Jet

The spreading rate S is given by,

$$S \cong \frac{d\eta_{1/2}(x)}{dx} \tag{5}$$

where the half-width variable ($\eta_{1/2}$) is defined as the radial position where the jet velocity reaches half of the centerline velocity at the same axial downstream distance. Another important test for any experimental data is whether it satisfies the governing equations. For an axisymmetric jet in an infinite environment, the velocity moment (M_0) profile must satisfy the momentum integral given, to second order by,

$$2\pi\int_0^\infty \left[U^2 + \overline{u^2} - \frac{1}{2}(\overline{v^2} + \overline{w^2}) \right] r\,dr = M_0 \tag{6}$$

where u is the velocity fluctuation on the axial direction and v *e* w are the radial velocity fluctuation. As suggested by Hussein et al (1993), for a first-order analysis, the integrated momentum balance can be discussed in terms of the contribution due to the velocity profile of the main flow fitted by a Gaussian curve passing through the jet half-width. Integrating Eq. 6 and ignoring the second-order terms yields (Eq. 7):

$$\frac{M}{M_0} = 2\pi\int_0^\infty \left[\frac{U}{U_0}(\eta)\eta d\eta \right] = \frac{\pi}{2A}\left(S\frac{2B_u}{\pi^{1/2}} \right)^2 = 2{,}27(S\frac{2B_u}{\pi^{1/2}})^2 \tag{7}$$

$$A = -\ln(0{,}5) \tag{8}$$

The values obtained by Hussein et al (1993) and the data mentioned by him from other experimentalists, as well as our own results, are summarized in Table 2.

.

Table 2 – Spreading rate and decay of a turbulent round jet

Autor	Measurement Technique	Re	S	B_u	X_0 [mm]	M/M_0
Wygnanski and Fiedler (1969)	HWA	100 000	0,086	5,7	3,0D	69%
Hussein et al. (1994)	HWA	95 500	0,102	5,9	2,7D	106%
Hussein et al. (1994)	LDA	95 500	0,094	5,8	4,0D	85%
Froening et al. (2013)	**HWA**	**35 300**	**0,105**	**4,5**	**6,9D**	**83%**

ISSN 2176-5480

3.2 Baseline and Chevron Nozzle Comparison

Bridges and Brown (2002) and Callender et al (2010) studied the influence of geometric parameters of chevron nozzles on the acoustic field and flow field. They found the penetration to be the most important parameter controlling mixing in the shear layer and vorticity, which is acknowledged as a determinant factor for the acoustic field. The effects on the flow field reported by them were mainly a shortening of the potential core, which seemed to be responsible for the decrease in intensity at low frequency, and a larger spreading rate at the beginning of jet. They also concluded that the increase in mixing led to an increase of the high frequency turbulence content. Experiment B aimed to evaluate changes in the flow field introduced by a chevron nozzle. Figure 8 shows the centerline velocity and turbulence intensity as a function of the downstream position.

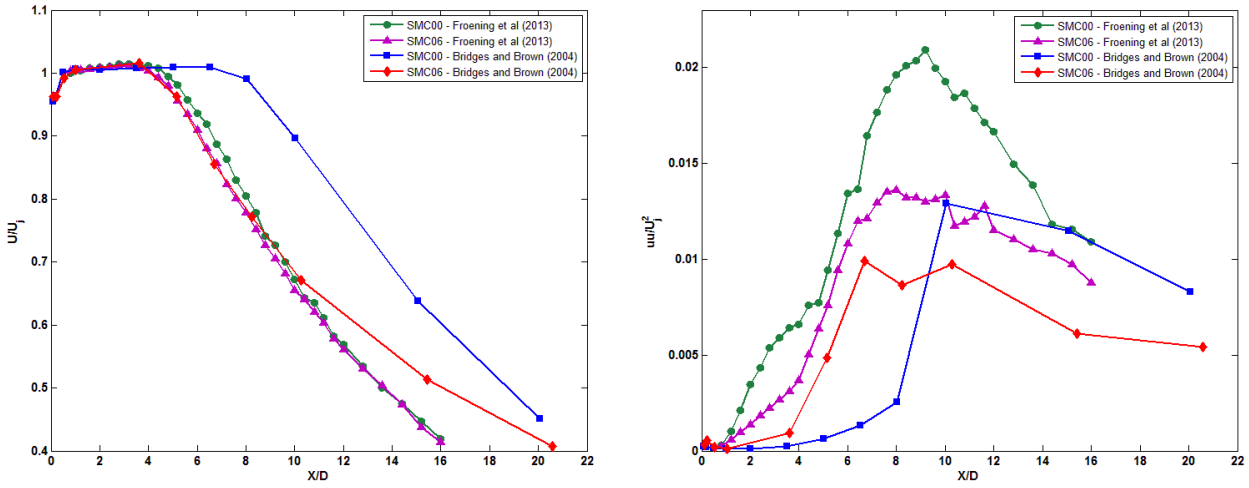

(a) Centerline velocity decay (b) Turbulence Intensity

Figure 8 – A comparison from SMC000 and SMC006 nozzles data from Bridges and Brown (2002) at Mach 0.9 and Froening et al. (2013) at Mach 0.13

The graph shows that the centerline velocity decays slightly faster with the chevron nozzle at Mach 0.13, especially between 6 *D* and 8 *D*. Inside the potential core, the jet is still coherent and therefore the level of the turbulence intensity is smaller. By the end of potential core (~4,5 *D*) the turbulence intensity grows up to four times faster for both nozzles. The peak in turbulence intensity is located around ~8 *D* downstream of the chevron nozzle (Exp. B) and ~9,5 *D* downstream for the baseline case (Exp. A). One can note that the effects on the flow caused by the chevrons are much more intense to the high speed jet.

Figure 9 shows a comparison of the velocity and turbulence intensity between the two nozzles at different axial distances downstream. The basis of the velocity profile to SMC006 is increased because the chevron nozzle diameter is greater than the baseline nozzle diameter, measured valley to valley. The figure shows that at the beginning and the end of the jet the turbulence intensity of the centerline are equal to both nozzles, however as the jet evolves along the main flow direction this difference increases (again the greatest differences are found at 8 *D*). Also should be noted, that at this velocity, the turbulence intensity level is higher to SMC000 at almost all positions. Finally, as Bridges e Brown (2002) also reported, at a sufficient distance the similarity theory can be applied even to the serrated nozzle, and both the jets tend to forget their initial conditions and develop a very similar profile

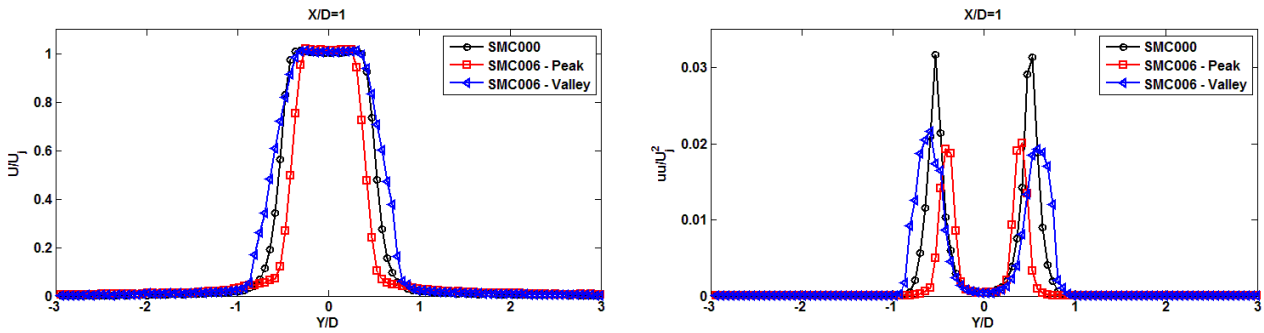

ISSN 2176-5480

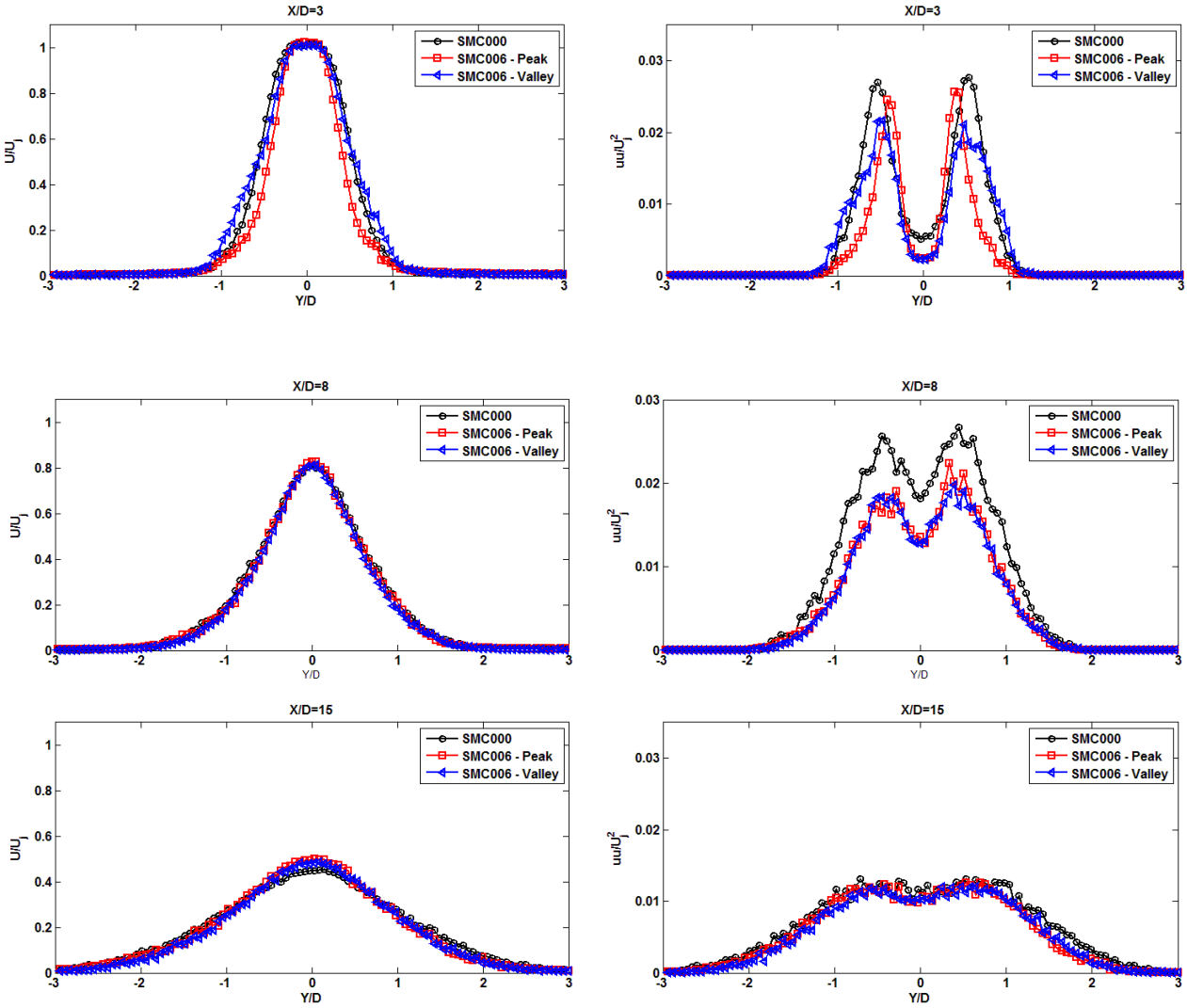

Figure 9 - Velocity and turbulence intensity profiles (X/D=1; X/D=3; X/D=8 and X/D=15).

Figure **10** we see centerline spectra for the baseline nozzle and the chevron nozzle at several downstream positions. At X/D=1 both spectra show high wavenumber content related to signal noise. Several peaks can be observed in the low wavenumber range, with a pronounced peak at approximately 60 Hz. This could be noise related to the power grid, but at this point we are not sure. For both nozzles we see a full transition to the expected one-dimensional energy spectrum with a clear -5/3 inertial subrange by X/D=30. Qualitatively both spectra show similar downstream evolution.

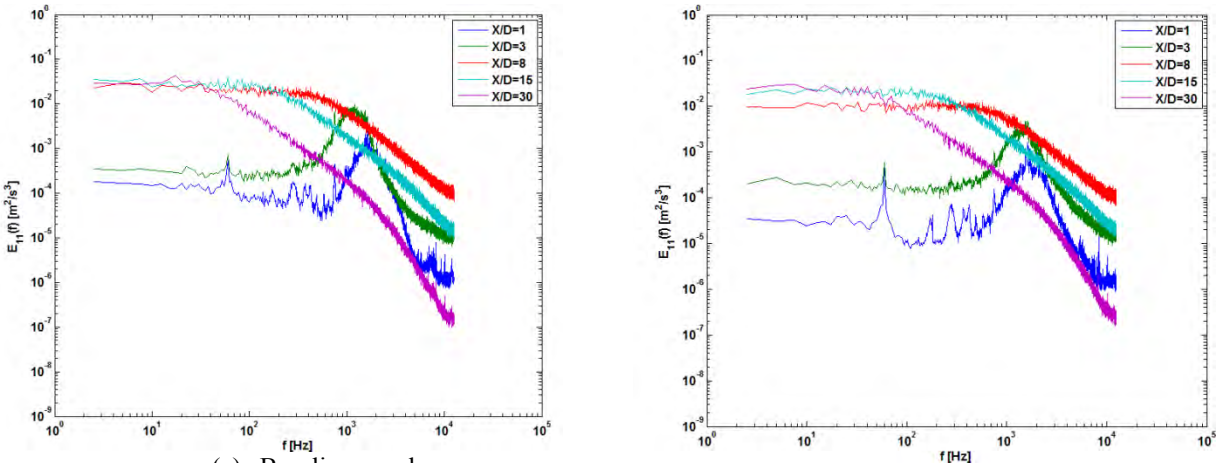

(a) Baseline nozzle.

(b) Chevron nozzle.

ISSN 2176-5480

Figure 10 – One-dimensional turbulent kinetic energy spectra at jet centerline for several downstream positions.

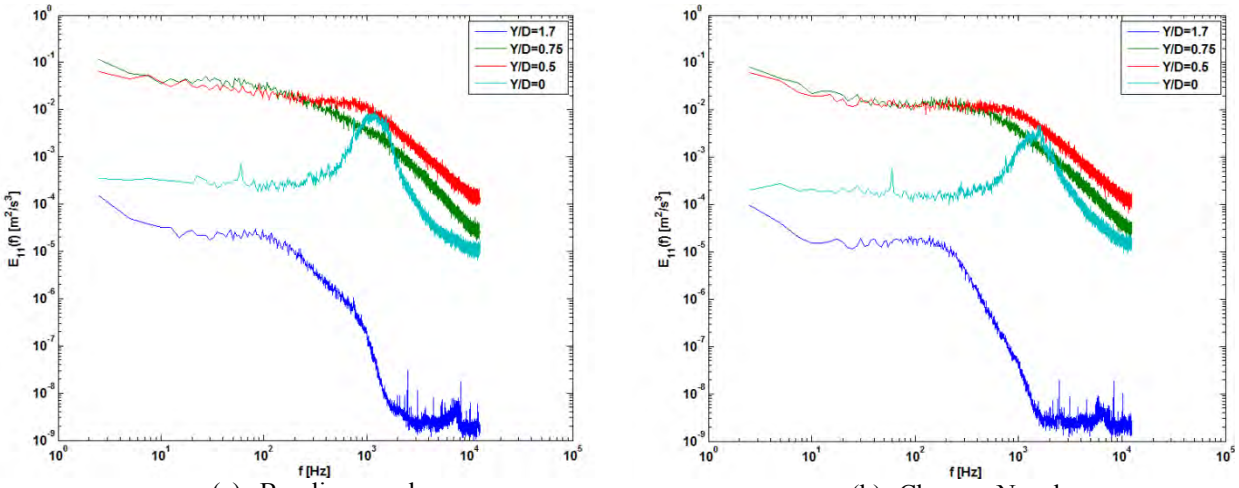

(a) Baseline nozzle. (b) Chevron Nozzle.

Figure 11 - One-dimensional turbulent kinetic energy spectra for several radial positions at X/D=3.

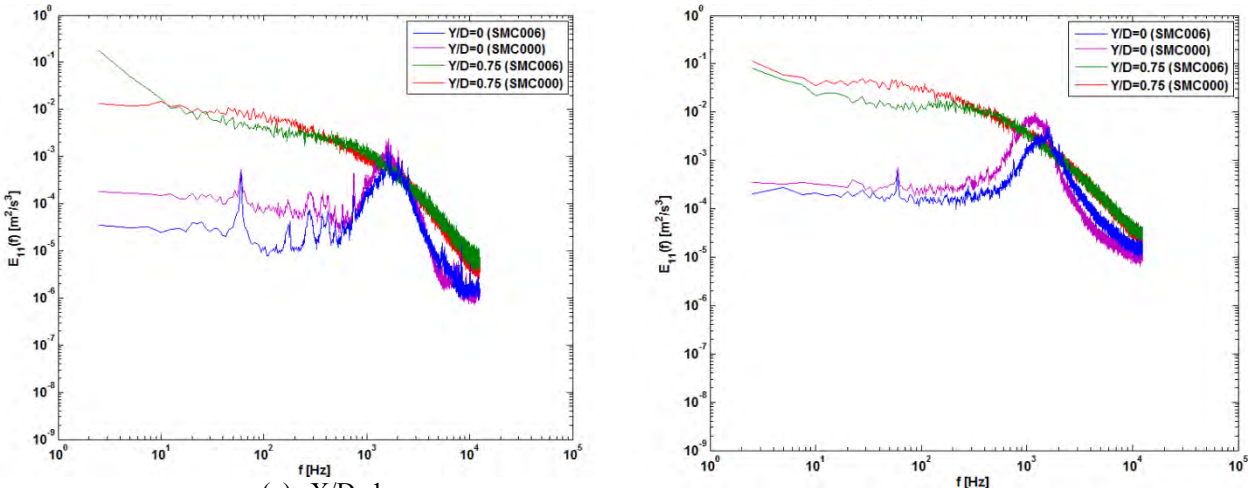

(a) X/D=1 (b) X/D=3

Figure 12 – Nozzle comparison of one-dimensional turbulent kinetic energy spectra for two radial positions at (a) X/D=1 and (b) X/D=3.

Figure 11 shows the one-dimensional turbulent kinetic energy spectra for four radial positions at X/D=3. For the baseline nozzle (a), at Y/D=1.7, a timid inertial range seems to be developing, which is absent for the chevron nozzle. This leads us to believe that the baseline nozzle has spread a bit further for this axial position. Indeed, this is the case as can be seen in the top left panel Figure 9 (peak).

Figure 12 shows one-dimensional turbulent kinetic energy spectra for both nozzles at two downstream positions. At X/D=1 the only significant difference is in the low-wavenumber content of the spectrum for the centerline position. At X/D=3 a perceptible shift towards higher wavenumbers can be seen in the chevron nozzle when compared to the baseline case.

4. CONCLUSIONS

The results shown here reveal a slight difference in the spreading rate and decay rate of both nozzles. Each class of laboratory jet is in principle asymptotically unique (e.g. top-hat jets, fully-developed pipe flow jets, etc.), and retain a dependence on the source Reynolds number (Hussein et al, 1994). Thus, the lower Reynolds number, in addition to

ISSN 2176-5480

specifics of nozzle geometry and flow generation used in these experiments, is a likely candidate for discrepancies found with respect to other jet experiments reported in the literature. Since the momentum balance is independent of the jet initial conditions, and the second order terms are not being considered, the value of 83% is in a good agreement with the theory and other experimental results.

When comparing nozzle geometry, previous experiments show that chevrons reduce the length of the potential core and the overall level of the turbulence intensity, in addition to shifting the peak closer to the jet exit. It is possible to note neither a high potential core reduction nor a high shift in the turbulence intensity was observed in our experiments. A possible interpretation of this result is that chevrons are not very effective as a noise reduction element when used in low speed jets. This is because the increase of turbulence intensity at the beginning of the jet development, indicating a high dissipation of the energy, is recognized as the main mechanism of jet noise reduction. However, in our experiments we have not actually made any acoustic measurements, therefore it remains to be seen if statement above is correct.

5. REFERENCES

Bridges, J. and Brown, C. A., 2004. *Parametrict testing of chevrons on single flow hot jets*. 10th AIAA/CEAS Aeroacoustic Conference, Cleveland,OH, (AIAA2004-2824).

Bridges, J. and Brown, C. A., 2005. *Validation of the Small Hot Jet Acoustic Rig for aeroacoustic research*. 11th AIAA/CEAS Aeroacoustic Conference, Cleveland,OH, (AIAA2005-2846).

Callender, B., Gutmark, E. J. and Martens, S., 2010. *Flow field characterization of coaxial conical and serrated (chevron) nozzles*. Exp Fluids (2010) 48:637-649.

DANTEC Dynamics, 2004. *StreamLine – Installation & User´s guide.* Dinamarca, 2004.

Engel, R. C., 2012. *Análise de modelos de previsão de escoamento e do ruído acústico de jatos subsônicos gerados por bocais serrilhados.* MSc. thesis, Universidade Federal de Santa Catarina, Florianópolis.

George, W. K., 1989. *The self-preservation of turbulent flows and its relation to initial conditions and coherent structures*. Advances in Turbulence, p.39-72, Hamisphere.

Hussein, J. H., Capp, S. P. and George, W. K., 1994. *Velocity measurements in high-Reynolds-number momentum-conserving, axisymmetric, turbulent jet*. Journal of Fluid Mechanics, Vol.258, no 8, p.31-75, Jan 1994.

Morris, P. J., Zaman and K. B. M. Q., 2010. *Velocity measurements in jets with application to noise source*. Journal of Sound and Vibration, 329 (2010) 394-414.

Pope S. B., 2000. *Turbulent Flows.* Cambridge University Press, Cambridge, United Kingdom,1st edition, 2000.

Silva, C. R. I., 2011. *Development of a novel RANS-based method for the computational aeroacoustics of high speed jets.* Ph.D. thesis, Universidade de São Paulo, São Paulo.

Wygnanski, I and Fiefler, H. E., 1969. *Some measurements in the self-preserving jet.* Journal of Fluid Mech., 38, 577-612.

6. RESPONSIBILITY NOTICE

The authors are the only responsible for the printed material included in this paper.